STScI | SPACE TELESCOPE SCIENCE INSTITUTE

Instrument Science Report WFC3 2017-02

Analysis of Dragon's Breath and Scattered Light Detector Anomalies on WFC3/UVIS

J. Fowler, L. Markwardt, M. Bourque, & J. Anderson

February 10, 2017

Abstract

We summarize the examination of the light anomalies known as Dragon's Breath and Scattered Light for the UVIS channel of Wide Field Camera 3 (WFC3) of the Hubble Space Telescope (HST). We present three methods for WFC3 users to help avoid these effects during observation planning. We analyzed all of the full-frame wide and long pass filters with exposure times ≥ 300 *seconds, comprising* $\sim 13\%$ *of WFC3/UVIS on-orbit data (*$\sim 20\%$ *of all full-frame data, and* $\sim 35\%$ *of all full-frame* ≥ 300 *second exposures.) We find that stars producing Dragon's Breath peak at specific orientations to the detector and V-band magnitudes. The bulk of these stars fall along the vertical and horizontal edges, within* ~ 490 *pixels of the image frame. The corners of the detector show significantly fewer instances of Dragon's Breath and Scattered Light, though still a few occurrences. Furthermore, matching stars outside the field of the image to V-band magnitude data from the Hubble Guide Star Catalog II (GSC-II) shows that stars causing the anomaly consistently peak around a V-band magnitude of* 11.9 *or* 14.6*, whereas the general trend of objects lying outside the field instead peaks around a magnitude of* 16.5 *within our exposure time and filter selection.*

Introduction

The Hubble Space Telescope (HST) Wide Field Camera 3 (WFC3) Instrument inevitably takes many images where stars lie immediately outside the image captured by

the detector. With some frequency ($\sim$ 12.5% of the analyzed images) these stars create a notable pattern of artificial light on the detector that has been termed 'Dragon's Breath' for its appearance as if something is breathing fire onto image. This effect is sometimes distinguished from 'Scattered Light' where the anomaly does not originate from the edge of the detector, but moving forward we will consider Dragon's Breath to include Scattered Light effects.

Figure 1 shows an example of both Dragon's Breath and Scattered Light on WFC3/UVIS. This effect presents itself in varying levels, some so subtle that they can be difficult to see visually, and others so dramatic they may adversely impact the ability to glean information from a science image.

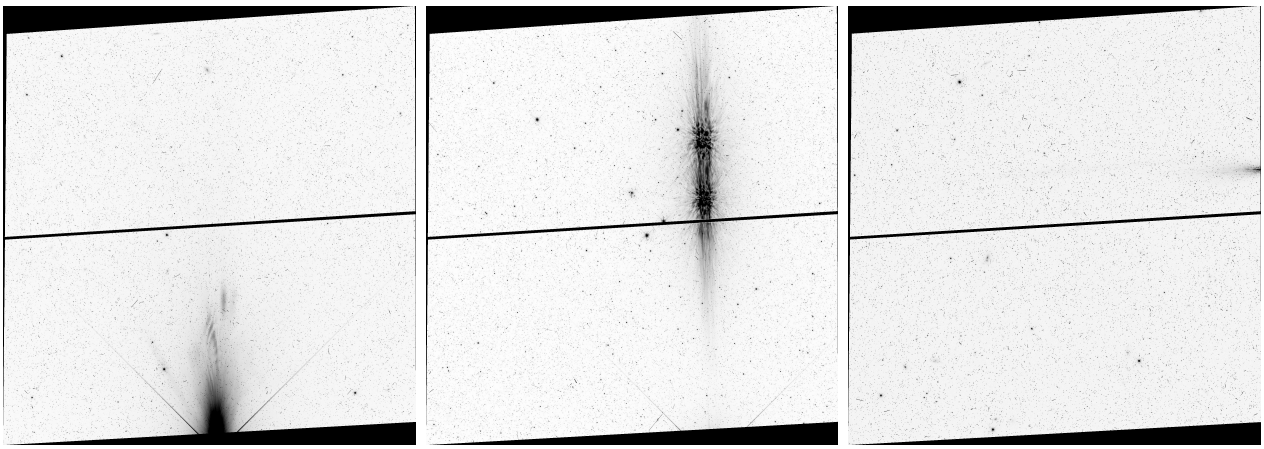

Fig. 1.—*Left: From the bottom of the image a prominent example of Dragon's Breath spills into the image. Middle: In this image a dramatic example of Scattered Light projects an effect into the middle of the detector image. Right: A more subtle example of Dragon's Breath from the top right, this resembles the bulk of Dragon's Breath effects.*

For a quantitative comparison of the effect of larger, smaller, and no Dragon's Breath anomaly, we compared three similarly sized regions; one region was entirely filled with a Dragon's Breath anomaly, one had a smaller anomaly that took up only a few pixels, and one that was just the background level of the image. Table 1 shows the comparative statistics for each of the three regions.

Effect	Pixels within Region	Mean Pixel Value	Median Pixel Value
Large Anomaly	1.0×10^6	130.5	59.6
Small Anomaly	1.1×10^6	44.9	29.2
No Anomaly	1.0×10^6	40.1	27.9

Table 1:*By comparing the counts in three regions, one entirely made up by an anomaly, one with a small anomaly, and one with just image background, we can quantitatively compare the impact of Dragon's Breath on an image.*

Dragon's Breath and Scattered Light are not new anomalies, but have been present

since the ground testing of WFC3, where a case of Scattered Light was traced back to an unpainted pinhole in the filter (Baggett et al., 2006). Furthermore, Dragon's Breath is not only specific to WFC3/UVIS; it also affects the Advanced Camera Survey/Wide Field Camera (ACS/WFC) and was also noticed during ACS ground testing (see discussion in Porterfield et al., 2016). The ACS team did a recent in-depth analysis of Dragon's Breath and Scattered Light, which inspires this work. Similarly, we have undertaken an effort to characterize under what conditions Dragon's Breath is most prevalent for WFC3/UVIS data, in hopes that WFC3/UVIS users may avoid unnecessarily compromising their their science data.

Data Analysis and Collection

Every on-orbit full-frame ≥ 300 second WFC3/UVIS exposure taken up to present with wide and long pass filters (11077 images total in the F606W, F814W, F600LP, F350LP, and F200LP filters) was visually inspected. Using the Two Micron All Sky Survey or 2MASS (Skrutskie et al., 2006) as a guide, we identified the positions of stars just beyond the UVIS field of view, allowing us to mark the locations of offending stars relative to the outer edge of the UVIS detector. The 2MASS coordinates were also used to match each object to a V-band magnitude from the Hubble Guide Star Catalog II or GSC-II (Lasker et al., 2008). From the image header, we were able to associate with each image an exposure time and observation date from the internal WFC3 Quicklook database (Bourque et al., 2016).

Analyzing the Beyond Images

It is non-trivial to determine which stars outside the image frame may be introducing artifacts into the image; this is especially the case when guide star position errors of a 0.5 $''$ radius prevent us from knowing the absolute registration from engineering data alone. To get a better registration, we must match stars in the image with known stars that have accurate coordinates in an absolute system. To do this, we use the 2MASS catalog and cross-identify stars in the image frame with catalog stars to determine the absolute mapping of the frame. This allows us to pinpoint the locations and brightnesses of catalog stars outside of the image frame. This procedure is similar to what was done for ACS in Porterfield et al., 2016, and it produces what we call a "Beyond" image, an example of which is shown in Figure 2. The Beyond image reproduces the original image along with a border, and the identified 2MASS stars as shown, both inside the image frame and outside.

Matching an anomaly and its star of origin required examining the Beyond images in an interface that allowed the analyst to match each Dragon's Breath effect to the most aligned star that matches the orientation of the anomaly. Alternatively, the analyst could mark the image as having no Dragon's Breath or being too crowded or distorted to be worthy of analysis. An object is marked as causing Dragon's Breath simply by clicking

the offending star. The interface records the clicked position, and matches it to the closest 2MASS object. The interface maintains a record of all the 2MASS stars within range of each image deemed worthy of analysis; data points that indicate the absence of Dragon's Breath are equally informative to this analysis as those that do trigger the anomaly. This procedure accumulates a lot of data – with many images having multiple stars within range when a Dragon's Breath or Scattered Light effect appears. Due to the difficult nature of visually inspecting several thousand images, the bulk of the data was processed twice, by two individuals (Fowler and Markwardt), in hopes of removing false classifications of the detector anomalies. The code that generates the Beyond images is unable presently to process images taken in subarrays, causing the restriction of the analysis to full-frame images.

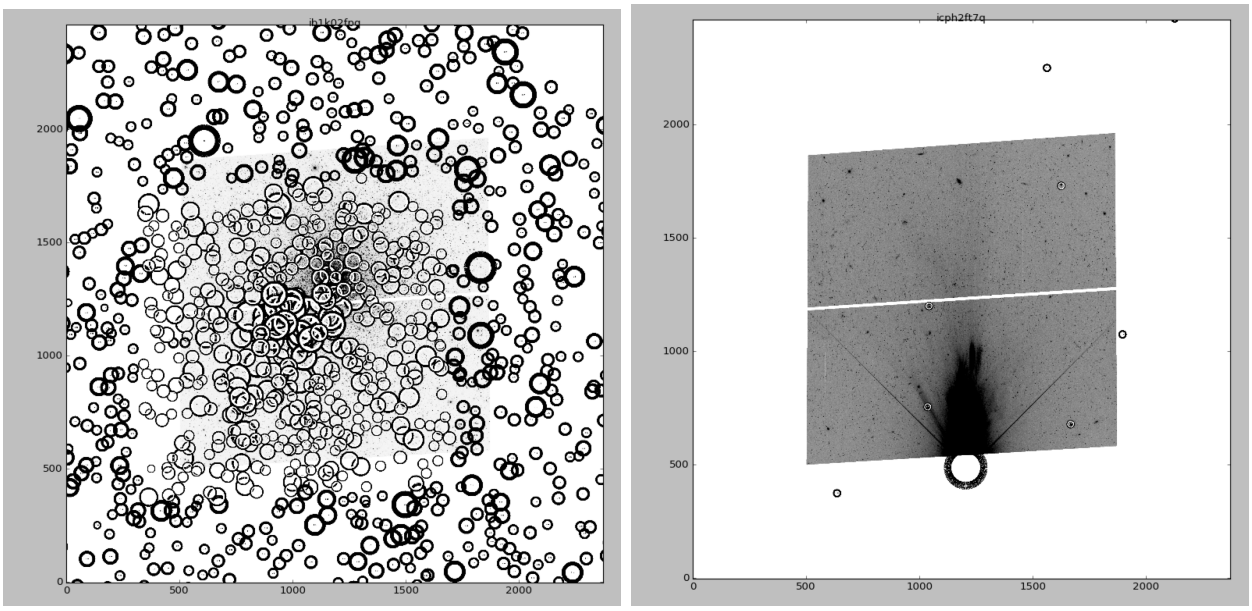

Fig. 2.—*Left: In this image the field is too crowded to accurately analyze the image. Right: Here the Dragon's Breath is obviously coming from the star immediately below the effect. In all Beyond images the size of the circle is dependent on the magnitude of the star.*

Collecting Additional Information

The 2MASS catalog lacks specifics of the UVIS data collection as well as any photometry that would compliment the fact that UVIS is a visible detector (2MASS has only IR photometry). Therefore, additional information was added to the data by querying from two sources – the publicly available GSC-II, and the internal only WFC3 Quicklook database. As GSC-II is presently available only through a web query form, we created a `Python` script to automate and emulate multiple web queries.

Every search was done with a 0.05° radius cone search, which returned between 20 and 100 objects for each set of coordinates. The closest object with an associated V-band magnitude was recorded, leaving all but 7% of the data with an associated magnitude. The process of automating the queries in `Python` is outlined in Appendix A.

Similarly, simply matching rootnames in Quicklook allowed the retrieval of any related information from the FITS header, specifically exposure time, observation date, and proposal ID were attached to the growing body of information. WFC3's Quicklook database can also be automatically queried in `Python`, which is described in Appendix B.

Analysis

In total 11077 images were examined; 1338 images were found to have been affected by Dragon's Breath. The specifics of each filter and its affected images are summarized in Table 2.

Filter	# Images Affected	# of UVIS Images	% Images Affected	% of Dragon's Breath
F606W	455	4821	10%	34%
F814W	443	5312	9%	33%
F600LP	36	518	7%	3%
F350LP	383	4218	9%	29%
F200LP	21	162	13%	2%

Table 2:*The above table breaks down how Dragon's Breath and Scattered Light affects each of the filters we analyzed. To get a better idea of how this is impacting the detector the table also includes what percent of WFC3/UVIS is made up by the given filter. (These statistics are without any images that used subarrays and have a* $\geq$ *300 second exposure time.)*

From here we endeavored to perform analysis that might isolate at what magnitudes, exposure times, detector electron counts, and positions these effects were prevalent. While there was some hope for areas of the detector that are free of Dragon's Breath, our analysis led to the conclusion that the immediate area $\sim$ 490 pixels around the detector is prone to Dragon's Breath effects with a few instances occurring beyond 490 pixels, as shown in Figure 3. There are also positions from the detector that are especially prone to the effect, which vary slightly by each image, as show in Figure 4. (As Figure 4 is difficult to match to specific positions Table 3 lists the positions corresponding to each peak.)

Aside from position, the Dragon's Breath objects are also more likely at two peak V-band magnitudes. Across all five analyzed filters, the data show two peaks within 0.5 magnitude of 11.9 and 14.6, even though the normal population of objects is peaking closer to 16.5, where the population of stars in the catalog continues to rise down to the faintness limit of the catalog. Figure 5 shows the histograms of stars outside the image frame with respect to magnitude. Filter F350LP does show a third more central peak around a magnitude of 13.4, but this peak is not reflected in the population of Dragon's-Breath-causing stars as a whole. Each histogram was fit to curve using the `gaussian_kde` package in `SciPy`. Table 4 lists the local maxima for each fitted curve and the corresponding magnitude. It must be mentioned that while all five filters peaking within 0.5 magnitude of each other is striking, there are

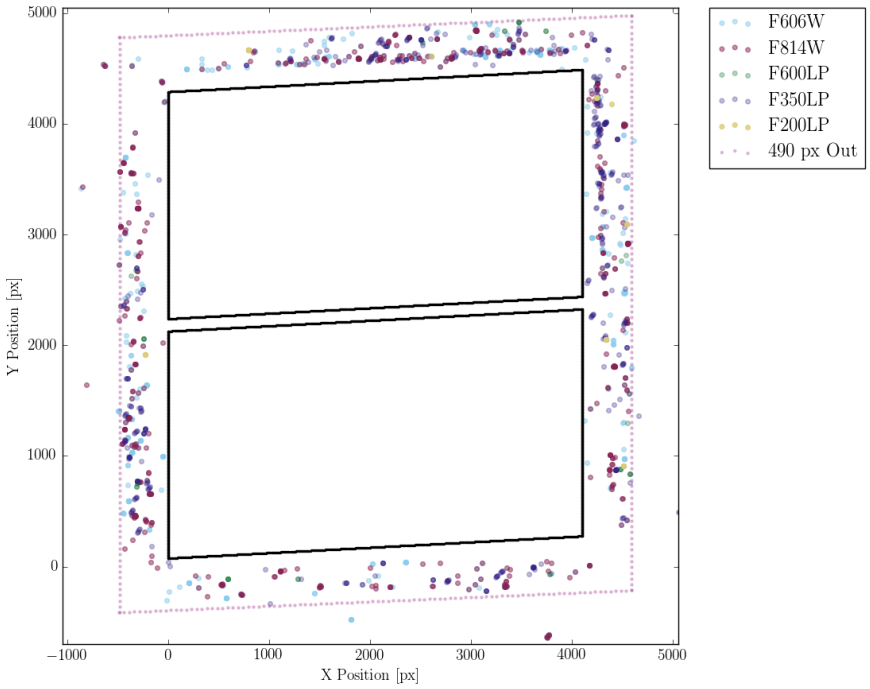

Fig. 3.—*This shows a top view of the Dragon's-Breath-causing and Scattered-Light-causing objects and their distance from the detector. The diagram is colored by filter, and shows two imprints – the solid that of the detector, and the lighter dotted outline is 490 pixels out, the region that contains the bulk of Dragon's Breath responsible stars.*

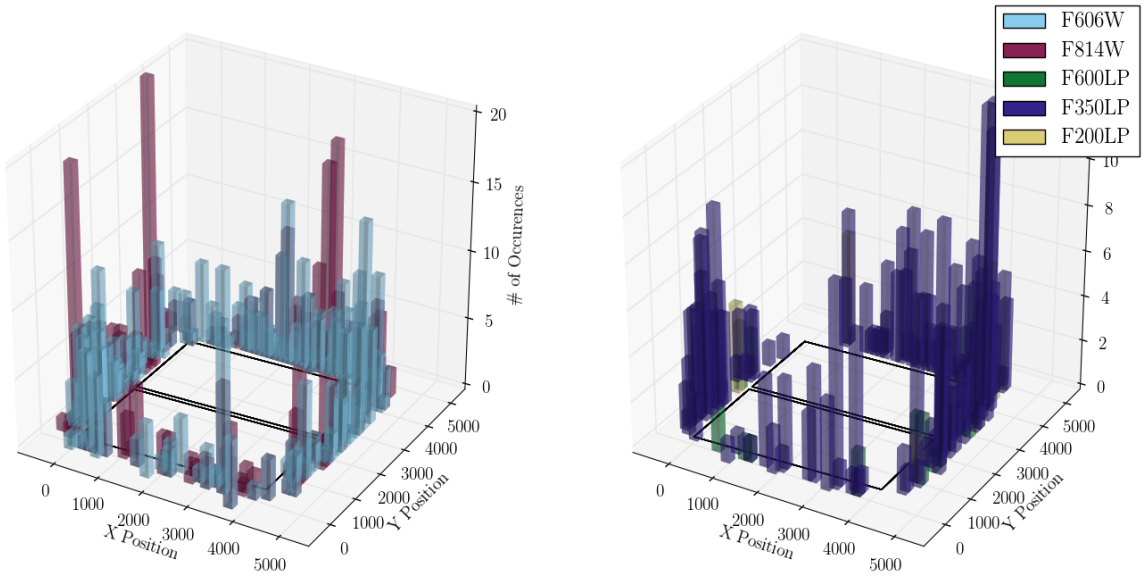

Fig. 4.—*These 3D histograms are with respect to detector orientation. While the specific values are difficult to read, they clearly show that each filter has one or more areas significantly more prone to Dragon's Breath. These peaks are enumerated in Table 3. Left: Wide Filters. Right: Long Pass filters.*

Filter	# Affected Images	Peak Center (px)
F606W	16	(3320.25,-279.75)
F606W	12	(3680.25,4640.25)
F606W	12	(2000.25,4520.25)
F814W	21	(4400.25,1760.25)
F814W	21	(-399.75,3200.25)
F814W	19	(-399.75,440.25)
F600LP	4	(560.25,-159.75)
F600LP	4	(3440.25,4880.25)
F600LP	4	(-399.75,680.25)
F350LP	13	(4160.25,3920.25)
F350LP	13	(4160.25,4160.25)
F350LP	12	(4280.25,3920.25)
F200LP	6	(4160.25,4160.25)
F200LP	5	(680.25,4640.25)

Table 3: *Each filter has its own major or minor peak in position. For F600LP and F200LP the statistics are sparse, though listing the positions explicitly shows some overlap between filters, for example* $(4160.25, 4160.25)$ *which peaks in F200LP and F350LP.*

2×10^4 more objects unaffected than affected, making definite comparisons more difficult.

In considering the peak magnitude of Dragon's-Breath-causing stars, a vital part of this consideration could also be the associated exposure time. While the V-band magnitude associated with each star is an intrinsic property of the object (unlike instrumental magnitude) the effective counts measured by the detector from each object outside of the frame is still dependent on exposure time. However, plotting the magnitude vs the exposure time, as well as looking at histograms of magnitude weighted by exposure time show no dependancies or comparable distributions as to these peaks in magnitude. These figures are shown in Appendix C. Furthermore, our selection of ≥ 300 second exposure times leaves the bulk of our exposures the same within a factor of two, so there should be little impact on the V-band magnitude of stars outside the image.

User Tools and Reccomendations

The goal of this extensive Dragon's Breath study was to make user tools and recommendations for avoiding Dragon's Breath in observations. The first hope was that there may be a region in which Dragon's Breath is less likely and turning the orientation of the observational field could potentially avoid Dragon's Breath. This was not found to be the case, though certainly some positions are more likely to allow Dragon's Breath (as enumerated in Table 3) and objects of more prone magnitudes should be avoided in these areas (as enumerated

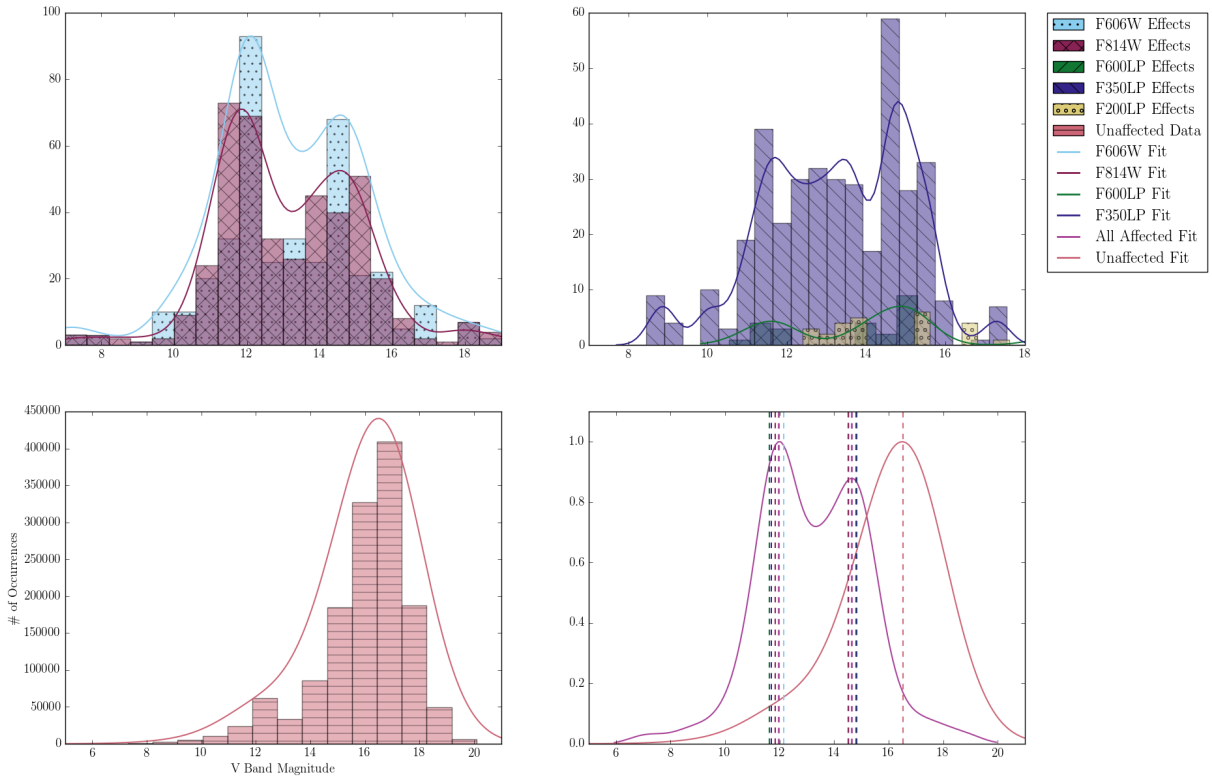

Fig. 5.—*Top Left:The population of objects causing Dragon's Breath effects for wide filters. Top Right: Dragon's Breath effects in long pass filters. (Due to so little data in filter F200LP, a fit curve has been neglected.) Bottom Left: The unaffected population of objects in the analyzed filters. Bottom Right: Fit curve for the total Dragon's Breath population and the unaffected objects scaled to one and dashed lines indicating the peaks of each fit curve thus far. Notice that every filter's stars peak around a magniutde of* 11.9 *and* 14.6*, whereas the general population of objects peaks closer to a magnitude of* 16.5.

Filter	Magnitude	Maxima
F606W	14.55	69
F606W	12.15	93
F814W	14.52	53
F814W	11.82	71
F600LP	14.83	7
F600LP	11.63	4
F350LP	14.80	44
F350LP	11.70	39
Unaffected	16.53	440686

Table 4: *The local maxima for each fit curve and corresponding magnitude. Note that each filter's peak is within* 0.5 *magnitude of* 11.9 *and* 14.6*. (Again, due to the small number of objects, filter F200LP is left out of this table.)*

in Table 4). But any object within a 490 pixel radius of the detector may potentially cause

Dragon's Breath. Furthermore, objects that peak around a V-band magnitude of 11.9 or 14.6 should be avoided in the immediate frame of the image if at all feasible.

Three user tools have been made to help plan observations, two of which are publicly available at the WFC3 Anomaly Page. Taking inspiration from the analysis of similar effects on the Advanced Camera Survey (ACS), we created an interactive `Bokeh` plot of Dragon's-Breath-causing stars with a mouseover preview of the affected image, as well as the V-band magnitude, exposure time, and observation date (Porterfield et al., 2016). Figure 6 shows an example of the user tool in use.

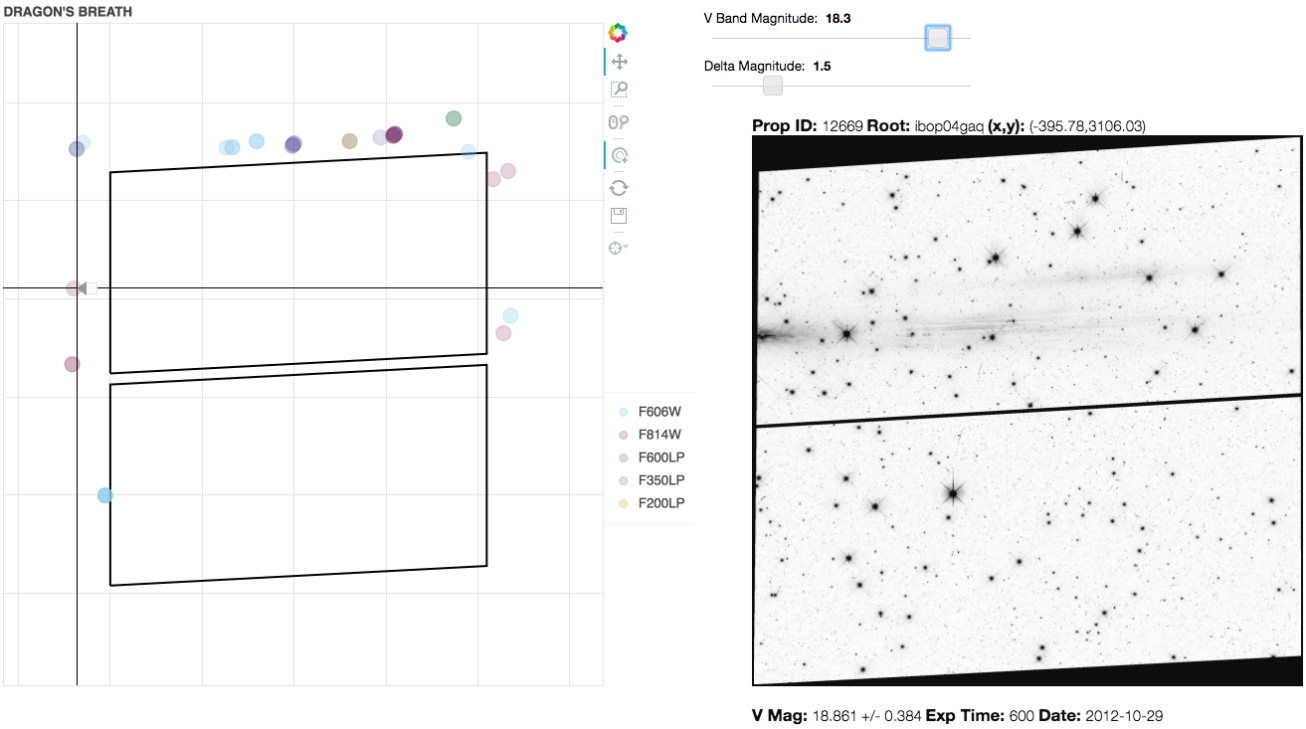

Fig. 6.—*The interactive plotting tool in use. The figure shows each Dragon's Breath effect, with interactive sliders on the top right that allow the user to filter for magnitude and the range of magnitude which appears. The mouseover on the right shows the image preview, as well as the proposal ID, root name, distance from detector, V-band magnitude with error, and observation date. This tool gives a visual way to see what potential observations might be vulnerable to Dragon's Breath.*

The other tool is a sortable and searchable table. The table contains every instance of analyzed Dragon's Breath, and the user can search the table for similar potential objects by filter, magnitude, or exposure time. This provides the same information as the interactive plot, but hopes to provide usage for those with a specific object in mind to avoid. Figure 7 shows an example of the table in use.

The third tool is an internal only tool, created as a plug in to `APT` and `Aladin` (McCullough, 2017). It allows the user to put their intended proposal in APT and catch objects that may fall into the 490 pixel zone of avoidance, and by viewing catalog overlays in APT,

Hello! You've found yourself a table of every cataloged star that causes Dragon's Breath for WFC3/UVIS. Each rootname links to a MAST preview if you want a look at how this particular image came out. Feel free to *root* around in the data, by searching for a few of the following parameters.

Search for Proposal IDs! | 14.5 | Search for Filter! | Search for Exposure Time!

Archive Preview Link	Proposal ID	Observation Date	V Band Magnitude	V Mag Error	Filter	Exposure Time	Position in (X,Y)
icze10u4q	14092	2016-6-22	14.5597	0.316179	F606W	348.0	(1455.35,4587.64)
icze10u3q	14092	2016-6-22	14.5597	0.316179	F606W	348.0	(1449.35,4578.82)
icze10u8q	14092	2016-6-22	14.5597	0.316179	F814W	373.0	(1467.17,4605.03)
ibdm02nbq	12019	2010-9-19	14.5127	0.215384	F814W	677.0	(2410.56,4599.96)
ibdm02n9q	12019	2010-9-19	14.5127	0.215384	F814W	681.0	(2408.07,4598.3)
ib4q07wpq	11524	2010-10-28	14.5285	0.342635	F600LP	677.5	(3327.07,4842.36)
ib4q07wrq	11524	2010-10-28	14.5285	0.342635	F600LP	677.5	(3327.07,4842.36)
ibeo1jlvq	12063	2011-5-22	14.5922	0.313052	F350LP	434.0	(-3.18,36.7)
icii36xzq	13633	2014-6-20	14.5714	0.451697	F350LP	370.0	(4153.93,2580.87)
icii36y1q	13633	2014-6-20	14.5714	0.451697	F350LP	370.0	(4158.41,2590.11)
icii27muq	13633	2014-6-18	14.5152	0.45116	F350LP	370.0	(4333.14,3070.81)
icii36xvq	13633	2014-6-20	14.5714	0.451697	F350LP	370.0	(4144.96,2562.41)
iciik1efq	13633	2014-10-16	14.5463	0.451407	F350LP	370.0	(4275.97,4429.51)
iciik0dkq	13633	2014-10-16	14.5463	0.451407	F350LP	370.0	(4249.92,4394.98)
iciik0dnq	13633	2014-10-16	14.5463	0.451407	F350LP	370.0	(4252.92,4398.91)

Fig. 7.—*This searchable table allows a user to search for filter, exposure time, or magnitude to isolate potentially troubling objects and make sure that no similar objects will be outside the frame of their intended proposal.*

a user can at least avoid objects in this zone which are at peak V-band Magnitudes.

Acknowledgements

Many thanks to Blair Porterfield and the ACS team for giving us a blueprint for Dragon's Breath analysis, Katie Gosmeyer for her help with mentoring and the SASP program, Sylvia Baggett for her keen insight on UVIS detector related issues, as well as Vera Platais for reviewing this ISR and providing invaluable feedback.

REFERENCES

Baggett, S. et al. 2006, Proc. of SPIE, 6265, 626532-2, "Filters for HST Wide Field Camera 3"

ISR 2016-06: ACS Cycle 24: Here There Be Dragons: Characterization of ACS/WFC Scattered Light Anomalies, B. Porterfield et al. 01 Nov 2016

Lasker, B. et al. 2008, AJ, 136, 735, "The Second-Generation Guide Star Catalog: Description and Properties"

Skrutskie, M. F. et al. 2006, AJ, 131, 1163, "The Two Micron All Sky Survey (2MASS)"

The Hubble Space Telescope Wide Field Camera 3 Quicklook Project, Bourque, Matthew, Bajaj, Varun, Bowers, Ariel, Dulude, Micheal, Durbin, Meredith, Gosmeyer, Catherine, Gunning, Heather, Khandrika, Harish, Martlin, Catherine, Sunnquist, Ben, Viana, Alex, ADASS 2016 (proceedings in press)

TIR 2017-01: Aladin Overlay of a Zone of Avoidance for Dragon's Breath, P. R. McCullough 2017 (in prep)

Appendix A

By creating a url for each query with a given RA, Dec, and 0.05° search cone, the data table was opened and the closest matching V-band magnitude data are selected. Figure 8 shows the `Python` code required to automatically query the GSC-II web portal. This was run twice to assure us that any points without data had sucessful queries.

```
def hgsc_query(ra, dec):
    # Build the url for the query
    url = 'http://gsss.stsci.edu/webservices/vo/CatalogSearch.aspx?RA=' + str(ra)
        + '&DEC=' + str(dec) + '&DSN=+&FORMAT=CSV&SR=' + str(.05) + '&CAT=GSC23'
    # See if the link is live and if so kidnap the v mag data
    try :
        dat = ascii.read(url)
        v_mag = dat['VMag']
        v_err = dat['VMagErr']
    # Otherwise, just set it to a value to catch later
    except (FileNotFoundError, urllib.error.URLError):
        v_mag = [-100]
        v_err = [-100]
    # And return it
    return v_mag, v_err
```

Fig. 8.—By emulating web queries and downloading .csv tables of each query, V-band magnitude and associated error were collected and added to the Dragon's Breath data.

Appendix B

Using `pyql`, a `Python` package built to interact with the Quicklook database, additional data on each image can be pulled from the FITS header by searching for the image by rootname. Figure 9 shows the `Python` code required to automatically query the WFC3 Quicklook database.

```
# Imports
from pyql.database.ql_database_interface import session
from pyql.database.ql_database_interface import Master
from pyql.database.ql_database_interface import UVIS_flt_0

def ql_query(rootname):
    # Query the QL database
    result = session.query(UVIS_flt_0.date_obs, UVIS_flt_0.proposid).\
             join(Master).\
             filter(Master.rootname == rootname).all()[0]
    # Parse data
    date = result.date_obs
    prop = result.proposid
    # Return each property
    return date, prop
```

Fig. 9.—By searching the Quicklook database for any matching rootname, and joining the FITS header data, the observation date and proposal ID are collected and added to the Dragon's Breath data.

Appendix C

Two additional figures – a plot of magnitude vs. exposure time (Figure 10) and a histogram of magnitude scaled by exposure time (Figure 11) show little if any trends in exposure time and specifically the relationship between magnitude and exposure time. The inclusion of these figures is in attempt to show that the peaks in V-band magnitude described above do not appear to be dependent on exposure time.

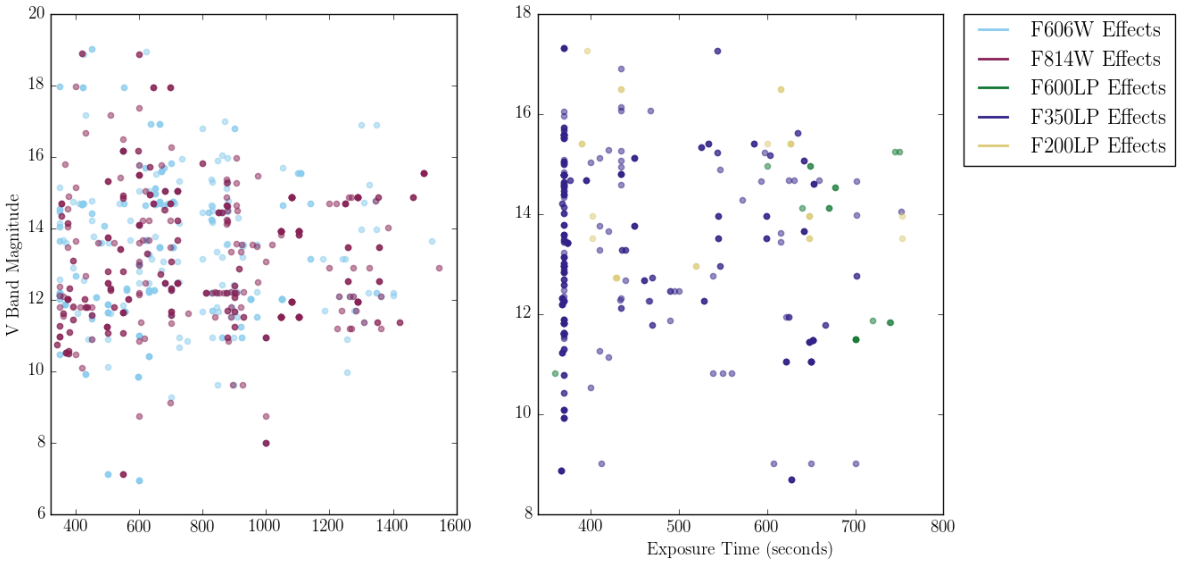

Fig. 10.—*Left: Dragon's-Breath-causing stars in wide filters. Right: Dragon's-Breath-causing objects in long pass filters. Neither set of filters seems to show a correlation in exposure time and magnitude that may belay a false trend in the magnitude peaks.*

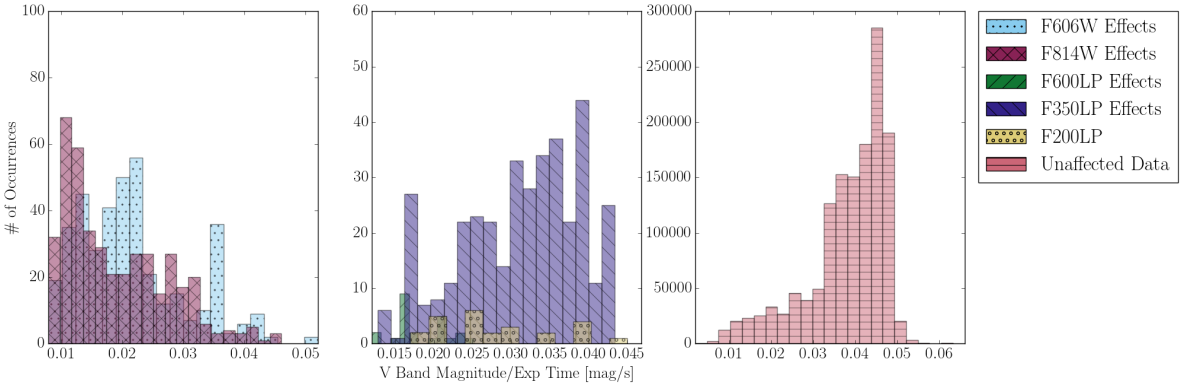

Fig. 11.—*Left: Dragon's-Breath-causing stars in wide filters. Center: Dragon's-Breath-causing objects in long pass filters. Right: The unaffected population of stars. Neither filter shows a notable peak.*